Available online at www.sciencedirect.com
ScienceDirect
Proceedings of the Combustion Institute 000 (2018) 1–8
Proceedings of the Combustion Institute
www.elsevier.com/locate/proci

On the determination of laminar flame speed from low-pressure and super-adiabatic propagating spherical flames

Mahdi Faghih [a], Zheng Chen [a,b,*], Jialong Huo [c], Zhuyin Ren [c], Chung K. Law [c,d]

[a] *SKLTCS, Department of Mechanics and Engineering Science, College of Engineering, Peking University, Beijing 100871, China*
[b] *Center for Applied Physics and Technology, BIC-ESAT, CCSE, Peking University, Beijing 100871, China*
[c] *Center for Combustion Energy, Tsinghua University, Beijing 100084, China*
[d] *Department of Mechanical and Aerospace Engineering, Princeton University, Princeton, NJ 08544, USA*

Received 4 November 2017; accepted 23 May 2018
Available online xxx

Abstract

The outwardly propagating spherical flame (OPF) method is popularly used to measure the laminar flame speed (LFS). Recently, great efforts have been devoted to improving the accuracy of the LFS measurement from OPF. In the OPF method, several assumptions are made. For examples, the burned gas is assumed to be static and in chemical equilibrium. However, these assumptions may not be satisfied under certain conditions. Here we consider low-pressure and super-adiabatic propagating spherical flames, for which chemical non-equilibrium exists and the burned gas may not be static. The objective is to assess the chemical non-equilibrium effects on the accuracy of LFS measurement from the OPF method. Numerical simulations considering detailed chemistry and transport are conducted. Stoichiometric methane/air flames at sub-atmospheric pressures and methane/oxygen flames at different equivalence ratios are considered. At low pressures, broad heat release zone is observed and the burned gas cannot quickly reach the adiabatic flame temperature, indicating the existence of chemical non-equilibrium of burned gas. Positive flow in the burned gas is identified and it is shown to become stronger at lower initial pressure. Consequently, the LFS measurement from OPF at low pressures is not accurate if the burned gas is assumed to be static and at chemical equilibrium. For super-adiabatic spherical flames, the burned gas speed is found to be negative due to the local temperature overshoot at the flame front. Such negative speed of burned gas can also reduce the accuracy of LFS measurement. It is recommended that the direct method measuring both flame propagation speed

* Corresponding author.
E-mail addresses: cz@pku.edu.cn, chenzheng@coe.pku.edu.cn (Z. Chen).

https://doi.org/10.1016/j.proci.2018.05.027

and flow speed of unburned gas should be used to determine the LFS at low pressures or for mixtures with super-adiabatic flame temperature.

Keywords: Laminar flame speed; Propagating spherical flame; Low-pressure; Super-adiabatic temperature

1. Introduction

The laminar flame speed (LFS), S_u^0, is defined as the speed at which a planar, unstretched, adiabatic, premixed flame propagates relative to the unburned gases [1]. LFS is a fundamental physicochemical property of a combustible mixture. The fundamental application of LFS varies from development of chemical kinetics and surrogate fuel models [2] to turbulent combustion modelling [3]. Currently, the outwardly propagating spherical flame (OPF) method is popularly used to measure LFS due to its well-defined stretch rate and its capability in measuring LFS at elevated pressures [4,5]. However, there are several factors affecting spherical flame propagation, which result in large discrepancies in LFS measured from the OPF method [5]. Efforts still need to be devoted to improving the accuracy of LFS measurement. Otherwise, LFS data with large uncertainty cannot be used to restrain the uncertainty of chemical models [5]. This study focuses on the chemical non-equilibrium of burned gas in low-pressure and super-adiabatic propagating spherical flames. The chemical non-equilibrium effects on the uncertainty of LFS measurement from the OPF method are quantified here.

Usually the OPF method is used to measure LFS at normal and elevated pressures. Recently, it has also been used at sub-atmospheric pressures [6–9]. However, at lower pressures, the flame becomes thicker and thus the burned gas inside the propagating spherical flame might not reach chemical equilibrium if the ratio between flame radius and flame thickness is not large enough [10]. As shown in the present study, such chemical non-equilibrium can induce non-static flow in the burned gas and thereby affects the accuracy of LFS measurement. Therefore, the first objective of this work is to investigate the chemical non-equilibrium effects at low-pressure propagating spherical flames and to quantify its influence on LFS determination.

Besides the low-pressure flames, chemical non-equilibrium also occurs in flames with super-adiabatic flame temperature (SAFT) phenomenon. SAFT appears in rich hydrocarbon premixed flames, in which the maximum temperature can greatly exceed the adiabatic flame temperature. The nature of SAFT has been explored by several groups through numerical simulation of premixed planar flames [11–14]. Liu et al. [14] studied the SAFT phenomena in different fuel-rich mixtures. They showed that the super-equilibrium concentrations of H_2O and hydrocarbon induces SAFT. Zamashchikov et al. [13] found that the degree of SAFT strongly depends on the equivalence ratio. They attributed the local temperature overshoot to the diffusion of H_2 from the reaction zone to the preheated zone. Unlike the conclusion of Ref. [13], Liu and Gülder [15] proposed that the deficiency of H radical at the end of major heat release zone is responsible for SAFT. In direct injection gasoline engines, local high equivalence ratio occurs frequently and thereby the SAFT phenomenon is expected to appear. In spherical flame experiments measuring the LFS of such kind of mixture, the SAFT phenomenon also occurs and it might affect the accuracy of LFS measurement. To our knowledge, there is no study on SAFT phenomenon in outwardly propagating spherical flames. Therefore, the second objective of this work is to study the chemical non-equilibrium effects in outwardly propagating spherical flames with SAFT.

Based on the objectives discussed above, outwardly propagating spherical flames at low pressures or with SAFT phenomenon are investigated numerically and experimentally. The chemical non-equilibrium effects on the accuracy of LFS measurement from the OPF method are quantified and interpreted. Methane is considered in this study. Nevertheless, the same conclusions can be drawn for other fuels. Syngas/air and n-heptane/air flames at low pressures are considered and the results are shown in the Supplementary Documents due to paper length limit.

2. Numerical and experimental methods and flame speed formulations

In simulation, both planar and spherical premixed flames are considered here. CHEMKIN-PREMIX code [16] is used to simulate the adiabatic, planar, premixed flame. The outwardly propagating spherical flames are simulated using the in-house code A-SURF [17–19]. The CHEMKIN package [20] is incorporated into A-SURF to calculate reaction rates and thermal and transport properties. For methane/air flames, we use GRI-Mech 3.0 [21] which was shown to work at sub-atmospheric pressures [22]. The mixture-averaged model is used to evaluate the mass

Please cite this article as: M. Faghih et al., On the determination of laminar flame speed from low-pressure and super-adiabatic propagating spherical flames, Proceedings of the Combustion Institute (2018), https://doi.org/10.1016/j.proci.2018.05.027

diffusivities for different species; and a correction term for diffusion velocity is included to ensure compatibility of species and mass conservation equations. Adaptive mesh refinement with the smallest mesh size of 16 μm is used. Grid convergence is achieved to ensure numerical accuracy. A-SURF has been successfully used in previous studies (e.g., [23–27]). The details on numerical schemes and code validation of A-SURF can be found in [17–19]. A-SURF is also used to simulate the transient planar flame propagation in an unconfined space, from which the reference unstretched LFS, $S^0_{u,ref}$, is obtained as:

$$S^0_{u,ref} = \frac{dx_f}{dt} - U_u \quad (1)$$

where U_u is the flow velocity of the unburned gas and x_f is the flame front position (defined as the position with maximum heat release rate).

Experiments for propagating spherical flames are conducted using the Generation-3 constant-pressure dual-chamber spherical flame apparatus at Tsinghua University [28]. Detailed specification of the experimental apparatus, procedure and data analysis were reported previously [28]. A large chamber with inner diameter of 12.5 cm allows large useful extrapolation ranges used in data processing [28]. The flame radius history, $R_f(t)$, is imaged using Schlieren photography and recorded with a high-speed digital motion camera (Photron Fastcam SA-Z) at 10,000 frames per second. The details on data processing are presented in [28].

For OPF, the flame propagation speed is equal to the time derivation of flame radius, i.e., $S = dR_f/dt$. The stretched flame speed relative to unburned gas is $S_u = S\text{-}U_u$, in which U_u is the flow speed of unburned gas at the flame front. In experiments, U_u can be measured through high-speed PIV [10,29,30]. Consequently, the LFS is determined through linear or nonlinear extrapolation between S_u and stretch rate, K, which is $K = 2S/R_f$ for OPF. Since both S and U_u are directly measured in experiments, this is called as the Direct Method (DM) [31].

An alternative method is first to obtain ${S_b}^0$ from extrapolation between S_b (the subscript b stands for speed relative to the burned gas) and K, and then to get LFS through ${S_u}^0 = \sigma^{eq} {S_b}^0$. Here σ^{eq} is the density ratio between the burned gas at chemical equilibrium and the unburned gas (i.e., $\sigma^{eq} = {\rho_b}^{eq}/\rho_u$). This method is based on the assumptions of static burned gas (i.e., $U_b = 0$ and thereby $S_b = S\text{-}U_b = S$) and chemical equilibrium of burned gas. It is called the Indirect Method (IM) since only S is measured and LFS is obtained indirectly [31].

Currently the DM is used only by Renou and coworkers [10], who are able to measure the unburned gas flow speed in OPF through high-speed PIV. All other groups use the IM. According to the discussion in the Introduction, chemical non-equilibrium in burned gas due to low pressure or SAFT might break the assumptions used in the IM, which affects the accuracy of LFS measured from the IM. This will be studied in the following two sections.

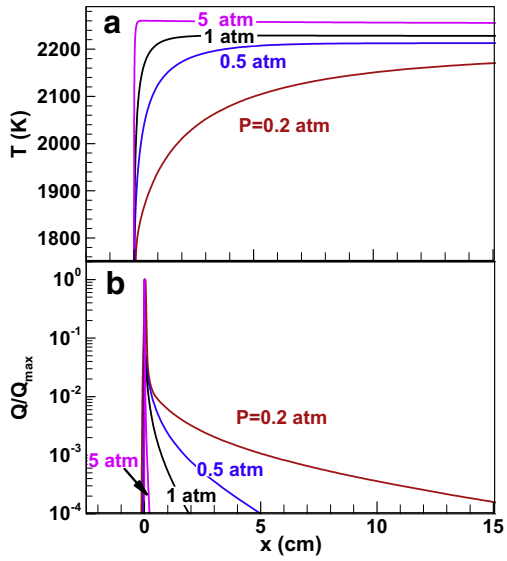

Fig. 1. Distributions of burned gas temperature (a) and normalized heat release rate (b) of 1D premixed planar flames in stoichiometric methane/air mixture at $T_u = 298$ K and different pressures.

It is noted that there are several factors affecting the uncertainty in LFS measured from the IM [5]. In this study, we focus on the influence of chemical non-equilibrium due to low pressure or SAFT. Therefore, other factors such as ignition, confinement, radiation and flame instability (reviewed in [5]) are not considered here.

3. Flames at sub-atmospheric pressures

We first consider spherical flame propagation at sub-atmospheric pressures. Figure 1 shows the distributions of burned gas temperature and normalized heat release rate of premixed planar flames in stoichiometric methane/air at different initial pressures. At $P = 5$ atm, the reaction zone is very thin (less than 2 mm) and the burned gas quickly reaches the adiabatic flame temperature, indicating that chemical equilibrium is quickly reached in burned gas. However, at sub-atmospheric pressure of $P = 0.5$ and 0.2 atm, the heat release zone becomes much wider and the adiabatic flame temperature is not immediately reached in burned gas. Therefore, at low pressures, the burned gas close to the flame front cannot reach chemical equilibrium. Even for atmospheric pressure, it takes about 3 cm for the burned gas to reach the equilibrium temperature.

Please cite this article as: M. Faghih et al., On the determination of laminar flame speed from low-pressure and super-adiabatic propagating spherical flames, Proceedings of the Combustion Institute (2018), https://doi.org/10.1016/j.proci.2018.05.027

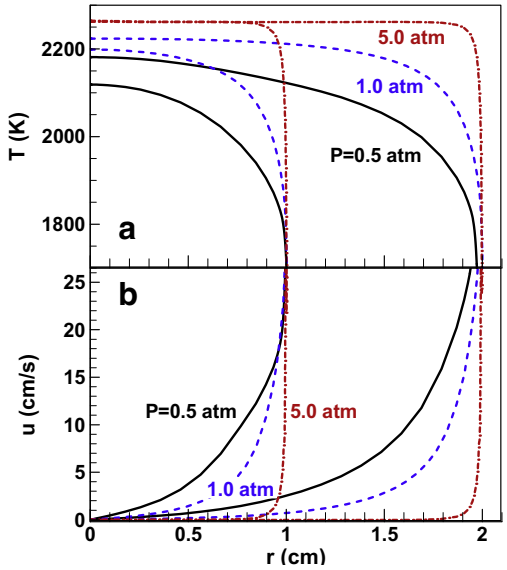

Fig. 2. Distributions of temperature (a) and flow speed (b) of burned gas in propagating spherical methane/air flames at $\phi = 1.0$, $T_u = 298$ K and different initial pressures. Only the results for flame radii around $R_f = 1$ cm and $R_f = 2$ cm are presented.

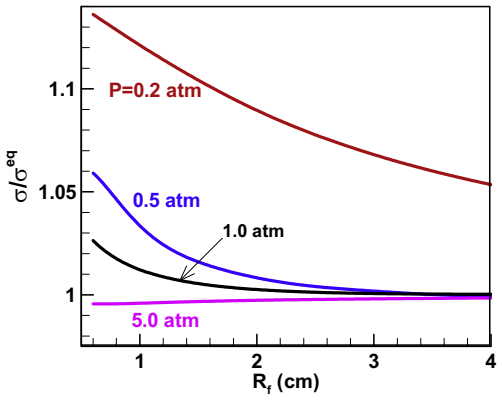

Fig. 3. Change of the normalized density ratio between burned and unburned gases with the flame radius. σ^{eq} is the density ratio at equilibrium; and $\sigma = \rho_b/\rho_u$ with ρ_b being the burned gas density at the center of the spherical flame.

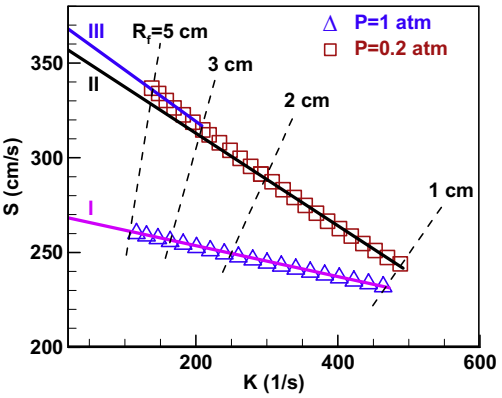

Fig. 4. Flame propagation speed as a function of the stretch rate for propagating spherical methane/air flame at $\phi = 1.0$, $T_u = 298$ K, and $P = 0.2$ and 1 atm. The symbols denote simulation results. The solid lines stand for linear fitting. And the dashed lines denote the flame radii contours (they are straight lines since $R_f = 2S/K$).

To assess how the chemical non-equilibrium affects spherical flame propagation, we conduct simulations for stoichiometric methane/air at $T_u = 298$ K and different pressures. The distributions of temperature and flow speed of burned gas are shown in Fig. 2 for flame radius around $R_f = 1$ and 2 cm. Similar to results shown in Fig. 1(a), the adiabatic flame temperature is not immediately reached in burned gas. At $P = 0.5$ atm, the adiabatic flame temperature of $T_{ad} = 2212$ K is never reached for $R_f = 2$ cm. Even at $P = 1$ atm, the distance to reach the equilibrium temperature is above 0.5 cm. Consequently, positive speed in burned gas is observed in Fig. 2(b) for both $P = 0.5$ and 1 atm. The burned gas speed is above 10 cm/s for $P = 0.5$ atm. Therefore, the assumption of static burned gas use in the IM does not hold for propagating spherical flames at sub-atmospheric pressures.

For the IM, the density ratio at equilibrium, $\sigma^{eq} = \rho_b{}^{eq}/\rho_u$, is used to obtain the $S_u{}^0$ from $S_b{}^0$. However, the density ratio cannot reach the equilibrium value if the burned gas is not in chemical equilibrium. Figure 3 compares the normalized density ratio for different pressures. Significant deviation of the density ratio from its equilibrium value is observed. The deviation increases greatly with the decrease of pressure or flame radius. For $P = 0.2$ atm, σ/σ^{eq} is around 1.1 for $1 \le R_f \le 2$ cm; and thereby about 10% under-prediction of $S_u{}^0$ is caused by using σ^{eq}. Therefore, the use of equilibrium density ratio in the IM can result in large uncertainty in LFS measurement at low pressures.

Figure 4 depicts the change of flame propagation speed with the stretch rate for $P = 0.2$ and 1 atm. At $P = 1$ atm, the linear trend between flame propagation speed, S, and stretch rate, K, is consistent throughout the flame radius range of $1 \le R_f \le 5$ cm. However, at $P = 0.2$ atm, the S-K slope changes with flame radius range: solid line II (which is linear fitting for $1 \le R_f \le 2$ cm) has smaller slope than solid line III (which is linear fitting for $3 \le R_f \le 5$ cm). Consequently, the low pressure LFS determined from the IM using σ^{eq} depends on the flame radius range used in extrapolation. This is demonstrated in Fig. 5, which shows

Please cite this article as: M. Faghih et al., On the determination of laminar flame speed from low-pressure and super-adiabatic propagating spherical flames, Proceedings of the Combustion Institute (2018), https://doi.org/10.1016/j.proci.2018.05.027

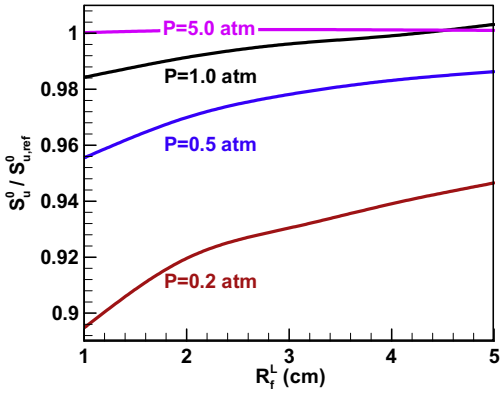

Fig. 5. Extracted laminar flame speeds from different flame radius ranges of $[R_f^L,\ R_f^L + 1\,\text{cm}]$ for methane/air flames at $\phi = 1.0$, $T_u = 298$ K and different pressures. The IM is used. $S^0_{u,ref}$ is the laminar flame speed of unstretched planar flame.

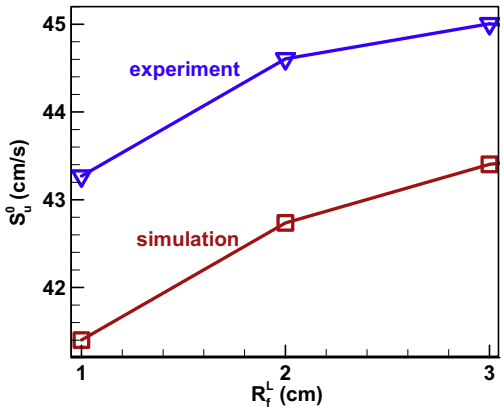

Fig. 6. The LFS determined by experiments and simulations for different flame radius ranges of $[R_f^L,\ R_f^L + 1\,\text{cm}]$ for methane/air flames at $\phi = 1.0$, $T_u = 298$ K and $P = 0.5$ atm. The IM is used.

the change of normalized LFS with flame radius range used in extrapolation for different pressures. For $P = 5$ atm, accurate LFS is obtained and it is nearly independent of flame radius range used in extrapolation. However, the LFS is under predicted by 10.4%, 4.4% and 1.6% respectively for $P = 0.2$, 0.5 and 1 atm when the flame radius range of $1 \le R_f \le 2$ cm is used. Such under prediction decreases as the flame radius increases. This is because the density ratio converges to its value at large flame radius as shown in Fig. 3. However, due to the limit of combustion vessel size and pressure rise, usually the flame radius range of $1 \le R_f \le 2$ cm is used in data processing.

To validate the simulation results, experiments for stoichiometric methane/air at $P = 0.5$ atm are conducted. Figure 6 compares the results from

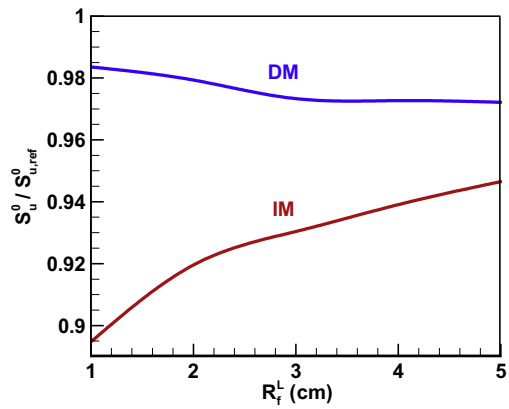

Fig. 7. Normalized LFS extracted from IM and DM and different flame radius ranges of $[R_f^L,\ R_f^L + 1\,\text{cm}]$ for methane/air flames at $\phi = 1.0$, $T_u = 298$ K and $P = 0.2$ atm.

simulation and experiments. The relative difference between experiments and simulations is within 4% and thereby is acceptable. The experimental results have the same trend as simulation results. Therefore, this confirms the influence of non-equilibrium density ratio and positive burned gas velocity in IM. Unfortunately, we cannot get experimental results at lower pressure of $P = 0.2$ atm. This is because at such low pressure the critical flame radius for successful ignition become very large, which greatly restricts the flame radius range that is uninfluenced by ignition [17,32].

The above results indicates that at low pressures, the IM cannot yield accurate LFS since the assumptions of zero burned gas speed and equilibrium density ratio are not satisfied. However, since such assumptions are not required in the DM, more accurate LFS can be obtained from the DM than that from the IM. This is demonstrated by Fig. 7. The relative discrepancy in S_u^0 obtained from the DM is shown to be within 2%. Therefore, the DM instead of IM should be used for low-pressure propagating spherical flames.

Figure 8 shows the normalized LFS extracted from IM and DM as a function of pressure. At sub-atmospheric pressures, the accuracy of the DM is much higher than that of the IM. At elevated pressures above 1 atm, the accuracy of the IM is slightly higher than that of the DM. Nevertheless, the accuracy of the DM is nearly independent of pressure and the relative under prediction in LFS is always within 2%.

In a brief summary, the above results indicates that at low pressures, the burned gas inside the propagating spherical flame might not be able to reach chemical equilibrium. Chemical non-equilibrium can induce non-static flow in the burned gas and make the density ratio to deviate from its equilibrium value. Consequently, the

Please cite this article as: M. Faghih et al., On the determination of laminar flame speed from low-pressure and super-adiabatic propagating spherical flames, Proceedings of the Combustion Institute (2018), https://doi.org/10.1016/j.proci.2018.05.027

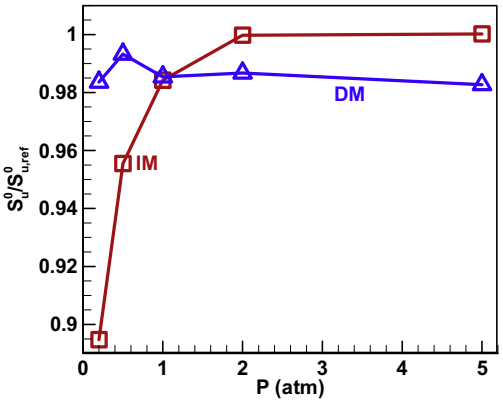

Fig. 8. Normalized LFS as a function of pressure for methane/air flames at $\phi = 1.0$ and $T_u = 298$ K. The flame radius range used in extrapolation is [1 cm, 2 cm].

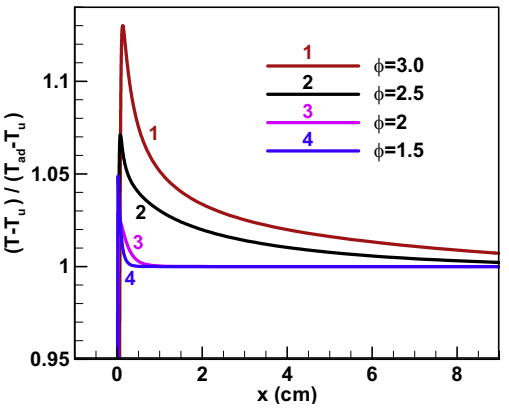

Fig. 9. Normalized temperature profile of premixed, planar methane/oxygen flames at $T_u = 300$ K, $P = 1$ atm, and different equivalence ratios.

accuracy of LFS measurement at low pressures is greatly reduced in the IM and the DM should be used.

4. Flames with super-adiabatic flame temperature

In this section we consider LFS measurement from propagating spherical flames with super-adiabatic flame temperature (SAFT). Methane/oxygen mixtures at $T_u = 300$ K and $P = 1$ atm and different equivalence ratios are considered.

According to Stelzner et al. [11], the super-adiabatic flames for methane/oxygen can be divided into two different regimes based on the equivalence ratio. In the first regime with $1 < \phi < 2$, the maximum super-adiabatic temperature occurs at $\phi = 1.5$. In this regime, the crucial factor for SAFT phenomenon is the maximum concentration of H radical and the combustion is very similar to the equilibrium condition. Figure 9 shows the normalized temperature profile for different equivalence ratios calculated by PREMIX. The temperature profiles for $\phi = 1.5$ and 2.0 are in consistent with those in Ref. [11]. The relative overshoot of the local temperature for $\phi = 1.5$ and 2.0 are respectively 5% and 2.5%. With further increase in the equivalence ratio, the consumption rate of H radical decreases and H radical overshoot occurs. The key factor for the second regime of $\phi > 2$ is the low consumption rate of H_2O in the super-adiabatic region [11]. Figure 9 shows that in the second regime, further increase in the equivalence ratio yields larger relative overshoot of the local temperature. The relative overshoot of the local temperature reaches 7% and 13% respectively for $\phi = 2.5$ and 3.0. Besides, for $\phi = 2.5$ and 3.0, the low consumption rate of H_2O results in a broad super-adiabatic region which is in chemical non-equilibrium. The readers

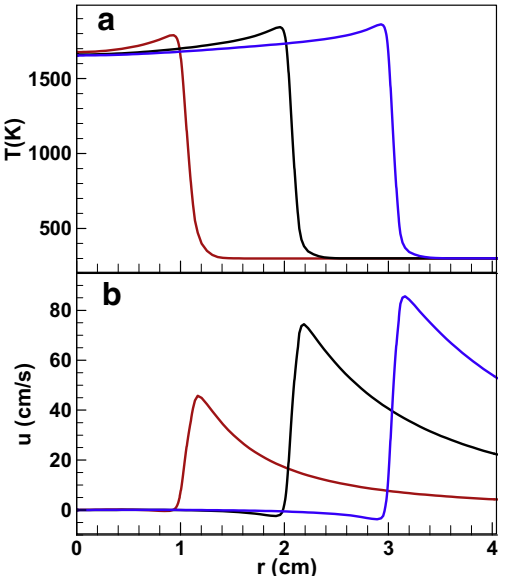

Fig. 10. The evolution of temperature (a) and flow speed (b) distributions in propagating spherical methane/oxygen flames at $T_u = 300$ K, $P = 1$ atm, and $\phi = 3$.

are referred to [11] for more details on how H_2O consumption rate influences the flame thickness in flames with SAFT.

Figure 10 shows the distributions of temperature and flow speed in propagating spherical methane/oxygen flames with $\phi = 3$. Due to the flame temperature overshoot, positive temperature gradient is observed for burned gas inside the spherical flame. As the burned gas becomes far from the flame front, its temperature gradually decreases toward the equilibrium value. Consequently, similar to spherical flames with strong

Please cite this article as: M. Faghih et al., On the determination of laminar flame speed from low-pressure and super-adiabatic propagating spherical flames, Proceedings of the Combustion Institute (2018), https://doi.org/10.1016/j.proci.2018.05.027

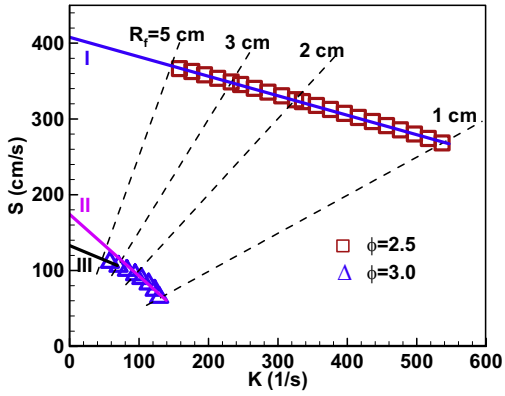

Fig. 11. Flame propagation speed as a function of the stretch rate for propagating spherical methane/oxygen flame at $\phi = 2.5$ and 3.0, $T_u = 300$ K and $P = 1$ atm. The symbols denote simulation results. The solid lines stand for linear fitting. And the dashed lines denote the flame radii contours (they are straight lines since $R_f = 2S/K$).

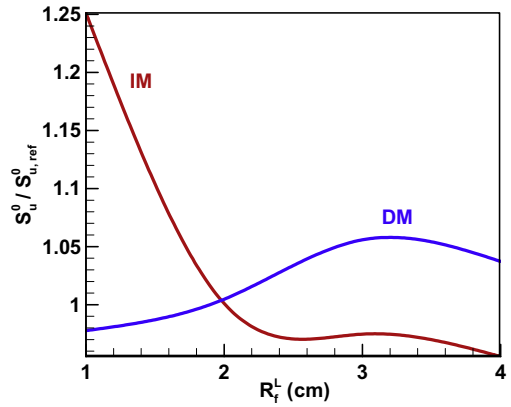

Fig. 12. Normalized LFS extracted from different flame radius ranges of $[R_f^L,\ R_f^L + 1\,\text{cm}]$ for methane/oxygen flames at $T_u = 300$ K, $P = 1$ atm and $\phi = 3$.

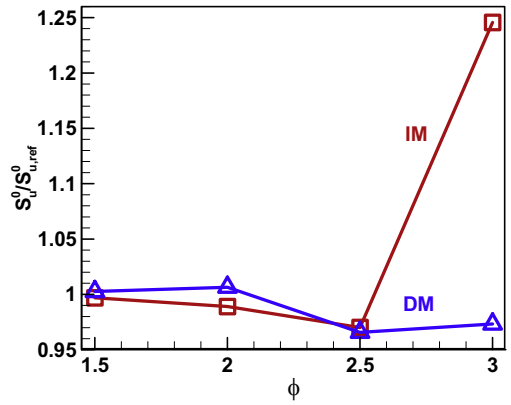

Fig. 13. Normalized LFS as a function of equivalence ratio for methane/oxygen flames at $T_u = 300$ K and $P = 1$ atm. The flame radius range used in extrapolation is [1 cm, 2 cm].

radiation effects [26,33–35], such positive temperature gradient can induce negative flow speed in the burned gas close to the flame front. This is observed in Fig. 10(b). Such negative speed of burned gas can reduce the flame propagation speed and thereby affects the LFS determination from the IM.

Figure 11 plots the flame propagation speed, $S = dR_f/dt$, as a function of stretch rate for CH_4/O_2 mixtures with $\phi = 2.5$ and 3. For $\phi = 2.5$, S changes linearly with K for the flame radius range of $1 \le R_f \le 5$ cm (solid line I). However, nonlinear change between S and K is observed for $\phi = 3$. The linear extrapolation based on flame radius range of $1 \le R_f \le 2$ cm (solid line II) and $3 \le R_f \le 5$ cm (solid line III) respectively yields the unstretched flame speed, $S_b{}^0$, of 175 cm/s and 133 cm/s. Therefore, the LFS obtained from the IM strongly depends on the flame radius range used in extrapolation for flames with strong SAFT.

Figure 12 compares the normalized LFS obtained from the IM and DM using different flame radius ranges for methane/oxygen mixture with $\phi = 3$. The LFS from the IM is over predicted for the flame radius range of $1 \le R_f \le 2$ cm. Such over prediction is shown to decreases when flames with larger radii are considered in data processing for the IM. This strong variation of LFS obtained from the IM can be described by the nonlinear behavior of S-K shown in Fig. 11. When the DM is used, the LFS is only under-predicted by 2% for the flame radius range of $1 \le R_f \le 2$ cm. Therefore, for CH_4/O_2 with $\phi = 3$ and strong SAFT, the LFS obtained from the DM is much more accurate than the IM. Figure 13 shows that the accuracy of the IM is close to that of the DM except the case of $\phi = 3$. For the IM, the deviation increases significantly when the equivalence ratio of $\phi = 3$ is reached. However, the accuracy of the DM is almost independent of equivalence ratios and the deviation is always within 4%. Therefore, for spherical flames with strong SAFT (here CH_4/O_2 with $\phi = 3$), the LFS obtained from the IM is not accurate and the DM should be used.

5. Conclusions

Numerical simulations considering detailed chemistry and transport are conducted for spherical flame propagation at low pressures or with super adiabatic flame temperature. The chemical non-equilibrium effects on the accuracy of LFS measurement from the OPF method are assessed. The main conclusions are:

Please cite this article as: M. Faghih et al., On the determination of laminar flame speed from low-pressure and super-adiabatic propagating spherical flames, Proceedings of the Combustion Institute (2018), https://doi.org/10.1016/j.proci.2018.05.027

(1) At sub-atmospheric pressures, the burned gas inside the propagating spherical flame cannot immediately reach chemical equilibrium and there exists a broad heat release zone. Such chemical non-equilibrium can induce positive flow in the burned gas and make the density ratio higher than its equilibrium value. Therefore at low pressures, the assumptions of static burned gas and chemical equilibrium condition used in the indirect method (IM) are not satisfied. It is recommended that the DM should be used for LFS measurement at low pressures. Besides, experiments are also conducted which confirm the simulation results.

(2) For super-adiabatic spherical flame propagation, negative flow in the burned gas is induced by local temperature overshoot and chemical non-equilibrium. Such negative speed of burned gas can reduce the flame propagation speed and thereby affects the LFS determination from the IM. Strong nonlinear dependence of propagation speed on stretch rate is observed for rich methane/oxygen mixture with strong SAFT phenomenon. It also shown that the accuracy of LFS measurement can be improved by using the DM rather than IM for mixtures with strong SAFT phenomenon.

Acknowledgments

This work is supported by National Natural Science Foundation of China (Nos. 91541204 and 91741126).

Supplementary materials

Supplementary material associated with this article can be found, in the online version, at doi:10.1016/j.proci.2018.05.027.

References

[1] G.E. Andrews, D. Bradley, *Combust. Flame* 18 (1972) 133–153.
[2] E. Ranzi, A. Frassoldati, R. Grana, et al., *Prog. Energy Combust. Sci.* 38 (2012) 468–501.
[3] N. Peters, *Turbulent Combustion*, Cambridge University Press, Cambridge, UK, 2000.
[4] F.N. Egolfopoulos, N. Hansen, Y. Ju, K. Kohse-Höinghaus, C.K. Law, F. Qi, *Prog. Energy Combust. Sci.* 43 (2014) 36–67.
[5] Z. Chen, *Combust. Flame* 162 (2015) 2442–2453.
[6] M.I. Hassan, K.T. Aung, G.M. Faeth, *Combust. Flame* 115 (1998) 539–550.
[7] F.N. Egolfopoulos, P. Cho, C.K. Law, *Combust. Flame* 76 (1989) 375–391.
[8] S. Yang, X. Yang, F. Wu, Y. Ju, C.K. Law, *Proc. Combust. Inst.* 36 (2017) 491–498.
[9] G. Dayma, F. Halter, P. Dagaut, *Combust. Flame* 161 (2014) 2235–2241.
[10] E. Varea, V. Modica, A. Vandel, B. Renou, *Combust. Flame* 159 (2012) 577–590.
[11] B. Stelzner, C. Weis, P. Habisreuther, N. Zarzalis, D. Trimis, *Fuel* 201 (2017) 148–155.
[12] V.S. Babkin, V.A. Bunev, T.A. Bolshova, *Combust. Explos. Shock Waves* 51 (2015) 151–159.
[13] V.V. Zamashchikov, I.G. Namyatov, V.A. Bunev, V.S. Babkin, *Combust. Explos. Shock Waves* 40 (2004) 32–35.
[14] F. Liu, H. Guo, G.J. Smallwood, Ö.L. Gülder, *Proc. Combust. Inst.* 29 (2002) 1543–1550.
[15] F. Liu, Ö.L. Gülder, *Combust. Flame* 143 (2005) 264–281.
[16] R.J. Kee, J. Grcar, M. Smooke, J. Miller, *Sandia Rep.* (1985) SAND85-8240.
[17] Z. Chen, M.P. Burke, Y.G. Ju, *Proc. Combust. Inst.* 32 (2009) 1253–1260.
[18] Z. Chen, *Combust. Flame* 157 (2010) 2267–2276.
[19] P. Dai, Z. Chen, *Combust. Flame* 162 (2015) 4183–4193.
[20] R.J. Kee, J. Grcar, M. Smooke, J.A. Miller, *Sandia National Laboratories Report* (1993) SAND89-8009B.
[21] G.P. Smith, D.M. Golden, M. Frenklach, et al., http://www.me.berkeley.edu/gri_mech/.
[22] B. Lefort, A. El Bakali, L. Gasnot, J.F. Pauwels, *Fuel* 189 (2017) 210–237.
[23] W. Zhang, Z. Chen, W. Kong, *Combust. Flame* 159 (2012) 151–160.
[24] H. Yu, Z. Chen, *Combust. Flame* 162 (2015) 4102–4111.
[25] P. Dai, Z. Chen, S. Chen, Y. Ju, *Proc. Combust. Inst.* 35 (2015) 3045–3052.
[26] Z. Chen, *Proc. Combust. Inst.* 36 (2017) 1129–1136.
[27] C. Qi, P. Dai, H. Yu, Z. Chen, *Proc. Combust. Inst.* 36 (2017) 3633–3641.
[28] J. Huo, S. Yang, Z. Ren, D. Zhu, C.K. Law, *Combust. Flame* 189 (2018) 155–162.
[29] S. Balusamy, A. Cessou, B. Lecordier, *Exp. Fluids* 50 (2011) 1109–1121.
[30] E. Varea, V. Modica, B. Renou, A.M. Boukhalfa, *Proc. Combust. Inst.* 34 (2013) 735–744.
[31] E. Varea, J. Beeckmann, H. Pitsch, Z. Chen, B. Renou, *Proc. Combust. Inst.* 35 (2015) 711–719.
[32] W. Zhang, X. Gou, Z. Chen, *Fuel* 187 (2017) 111–116.
[33] Z. Chen, *Combust. Flame* 183 (2017) 66–74.
[34] C. Xiouris, T. Ye, J. Jayachandran, F.N. Egolfopoulos, *Combust. Flame* 163 (2016) 270–283.
[35] H. Yu, W. Han, J. Santner, X. Gou, C.H. Sohn, Y. Ju, Z. Chen, *Combust. Flame* 161 (2014) 2815–2824.

Please cite this article as: M. Faghih et al., On the determination of laminar flame speed from low-pressure and super-adiabatic propagating spherical flames, Proceedings of the Combustion Institute (2018), https://doi.org/10.1016/j.proci.2018.05.027